International Ophthalmology **23:** 291–295, 2001.
J.R. Sampaolesi (ed.), Laser Scanning: Update 1, 109–113.

Scattering properties of the retina and the choroids determined from OCT-A-scans

H. Hammer, D. Schweitzer, E. Thamm, A. Kolb & J. Strobel
University of Jena, Department of Ophthalmology, Jena, Germany

Key words: OCT, tissue scattering, retina, choroid

Abstract

Goal: To determine the coefficient and the anisotropy of scattering as well as the refractive indices in the retina and in the choroid noninvasively *in vivo*. *Methods*: The power of coherent reflected light versus fundus depth is recorded in OCT-A-scans. The ratio of refractive indices is derived from the height of the reflection peaks. Provided that the absorption coefficient is known from fundus reflectometry, the scattering coefficient and anisotropy are calculated from the offset and the slope of the signal behind the reflection peaks on the basis of a single backscattering model. *Results*: We found scattering coefficients of 12/mm (retina) and 27.5/mm (choroid) as well as anisotropy values of 0.97 (retina) and 0.90 (choroid). *Discussion*: The OCT is usually employed for the measurement of intraocular distances. The new technique described here gives the unique opportunity to determine further interesting parameters of single ocular layers. The values given above are in good agreement with *in vitro* results.

Introduction

Recently, optical coherence tomography (OCT) is widely used to observe hidden morphologic structures in the depth of biological tissues. In the ophthalmology, OCT is used to obtain tomographic images of the ocular fundus. This enables the measurement of the thicknesses of retinal structures. However, coherent reflected light carries more information characterising the optical properties of tissue. The goal of this paper is to investigate the feasibility of OCT to determine the refractive index, the extinction coefficient, and the scattering anisotropy of tissues using a single backscattering model. This will be demonstrated at the example of an OCT-scan from a human ocular fundus *in vivo*.

Methods

OCT is an interferometric technique. Let us consider, e.g., a Michelson interferometer 7with a scattering sample in one arm and a mirror in the other one (reference arm). In order to avoid the superposition of many interfering waves backscattered from the sample, a light source with a high spatial but a short temporal coherence is used. This results in interference only if the optical path difference in both arms of the interferometer is not larger than the coherence length of the source [1]. If $L + \Delta L$ is the distance of the reference mirror and L that of the surface of the sample ($z = 0$) from the beam splitter (50/50), and if there is a reflection $R(z)$ in the depth z in the sample, at the detector the power [2, 3].

$$\begin{aligned} P(z) &= P_0 \times [(1 + R(z))/4 \\ &\quad +1/2\sqrt{R(z)} \times |\gamma(2(\Delta L - nz)/c)| \\ &= \times \cos(4\pi(\Delta L - nz)/\lambda)] \end{aligned} \quad (1)$$

is measured, where P_0 is the power of the light source, n is the refractive index of the sample, c is the velocity of the light, λ is the wavelength, and γ is the temporal coherence function.

As involuntary eye movements make it difficult to observe the interference between waves reflected from the eye and from a stationary mirror, Fercher et al. [4, 5, 6] used a dual beam interferometer: The light of the source is divided by an interferometer so that

there are two wavefronts with a path difference equal to the optical length of the eye incident on the eye. Thus, interference between the wave reflected at the cornea and that reflected at the ocular fundus is observed. In order to avoid losses of the signal resulting from the interference of a plane wave reflected at the fundus with a curved wave reflected at the cornea, a diffractive lens focusing 40% of the incident light at the cornea and 60% at the fundus is used. For this optical arrangement, Equation (1) has to be modified:

$$\begin{aligned} P(z)/P_0 \;=\; & 0.4R_c + 0.6R(z) + 2\sqrt{0.4R_c}\sqrt{0.6R(z)} \\ & \times|\gamma(2(\Delta L - nz)/c)| \\ & \times\cos(4\pi(\Delta L - nz)/\lambda). \end{aligned} \tag{2}$$

Here, R_c is the reflection at the cornea and $R(z)$ is the reflection at the fundus in the depth z. The interference term (third summand of Equation (2)) is separated from the incoherent power by shifting the reference mirror of the interferometer with a constant speed $v = \mathrm{d}L/\mathrm{d}t$ and filtering the detected signal with the Doppler frequency $f_D = v/\lambda$.

If $R(z)$ results from the scattering at cells and cell compartments for which the distance is shorter than the coherence length of the light source, the measured power results from a coherent summation over all scattered waves. To calculate this, the local distribution of the scatterers as well as the amplitude and the phase of their scattering function have to be known. Since this is difficult in biological tissues, a simple single scattering approach [3, 7] is used instead, making the following assumptions: The scatterers are randomly distributed in the sample and their distance is large compared to the wavelength. Only those photons contribute to the coherent signal, which reach the aperture of the detector after a single scattering event. The Stokes-vektor remained unchanged in this backscattering. In compliance, with these requirements we get for the mean power with the frequency f_D

$$\langle P(z)\rangle/P_0 = 2\sqrt{0.4\times 0.6\times R_c}$$

$$\times\sqrt{\int_{-\infty}^{\infty}\tilde{R}\times(\exp(-2\mu_t z')/CF)\times|\gamma(2n(z-z')/c)|^2\,\mathrm{d}z'}, \tag{3}$$

where $\tilde{R}$ is that fraction of light, which is scattered into the aperture of the detector [8]. The term CF is a correction of the power recorded from a scatterer in the depth z out of the focal plane in a confocal arrangement and is given by Yadlowsky [8] with

$$CF = (1-(z'-f)/f)^2 + ((z'-f)\pi r^2/\lambda f^2)^2, \tag{4}$$

where r is the radius of the laser beam in the pupil and f is the focal length of the eye. Thus, $\tilde{R}$ and the extinction coefficient μ_t were calculated solving the non-linear optimization problem

$$\sum_z |\tilde{P}(z) - 2\sqrt{0.4\times 0.6\times R_c}$$

$$\times\sqrt{\int_{-\infty}^{\infty}\tilde{R}\times\exp(-2\mu_t z')/CF\times|\gamma(2n(z-z')/c)|^2\,\mathrm{d}z'|^2}$$

$$\rightarrow \mathrm{Min} \tag{5}$$

by the use of Powell's conjugate direction set method [9]. Here, $\tilde{P}(z)$ is the measured coherent power versus depth normalized to the power of the incident beam. $\tilde{R}$ can be determined by the integration of the scattering phase function over the aperture angle of the observation. Assuming the Henyey–Greenstein phase function [10], we get

$$\tilde{R} = \frac{1}{4}\pi\times\int_{\pi}^{\pi+\varphi}(1-g^2)/(1+g^2-2g\,\cos\,\theta)^{2/3}\,\mathrm{d}\theta, \tag{6}$$

from which equation the anisotropy coefficient g of scattering can be calculated if the aperture angle φ = arctan(pupil radius/axial length of the eye) is assumed.

In OCT-scans of the ocular fundus (Figure 1), peaks resulting from specular reflection at the inner limiting membrane (ILM, border between vitreous and retina) and the retinal pigment epithelium (RPE) are observed. From the height of these peaks, the refractive indices of single layers may be determined using Equation (2) and Fresnel's reflection formula. For small angles of incidence of the laser beam onto cornea and retina, this results in

$$\frac{P}{P_0} = 2\sqrt{0.4\times 0.6}\times|(n_{\mathrm{air}}-n_{\mathrm{cornea}})/(n_{\mathrm{air}}+n_{\mathrm{cornea}})|$$

$$\times|(n_{\mathrm{vitreous}}-n_{\mathrm{retina}})/(n_{\mathrm{vitreous}}+n_{\mathrm{retina}})|. \tag{7}$$

Results

The coherent reflection at a human ocular fundus *in vivo* is given in Figure 1. This scan was recorded by

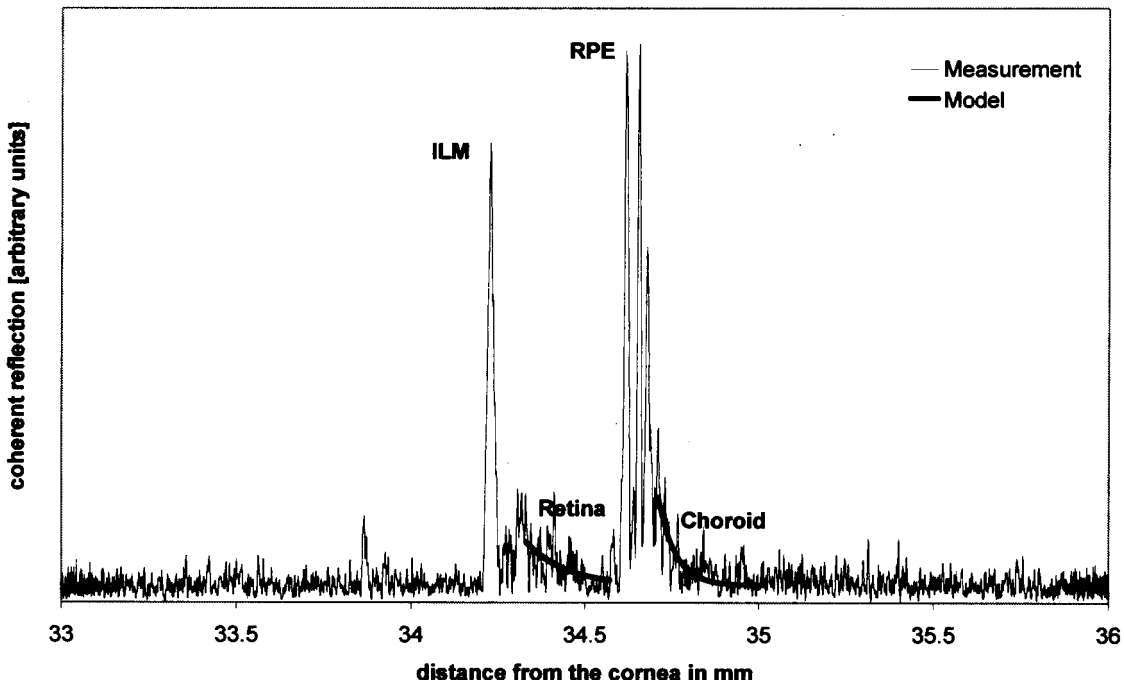

Figure 1. Measured OCT-scan through retina, RPE, and choroid as well as the calculated coherent power according to Equation (3) using the parameters given in Table 1.

Baumgartner et al. [11] using a dual beam interferometer. The light source was a superluminescent diode (C86142E, EG&G Optoelectronics, Canada) emitting at λ = 855 nm with a coherence length in air of 13 μm. The power of the beam in the pupillary plane was about 200 μW at a cross section of 0.6 $\times$ 0.8 mm^2. The coherence function γ was determined from the reflex of a glass plate.

Unfortunately, the data of Baumgartner et al. [11] were not given in power units. Therefore, it was impossible to calculate refractive indices. Equation (7) was employed for scaling the reflectance data using the refractive indices of Gullstrand's eye model [12]: $n_{\text{cornea}} = 1.376$, $n_{\text{vitreous}} = 1.336$, and n_{retina}=1.35.

$\tilde{R}$ and the extinction coefficient μ_t were determined solving the optimization problem Equation (5) and the scattering anisotropy g was obtained from Equation (6) for the retina (34.33–34.57 mm from the cornea) and for the choroids (34.71–35.01 mm from the cornea). In the calculation for the choroid, the incident power was corrected for the extinction $e^{-\mu_t z}$ of the retina. The reflected coherent power according to the single backscattering model Equation (3) is shown in Figure 1 and all data are given in Table 1.

To obtain an error measure (Table 1), we calculated the variation of one parameter ($\tilde{R}$ or μ_t) needed to obtain a value of the RMS deviation between measurement and model twice as high as the minimum, while the other parameter was kept constant at it's optimal value.

Discussion

The results in Figure 1 and Table 1 show that the single backscattering model, first employed in the interpretation of OCT-scans by Schmitt et al. [3], is applicable to scans from the ocular fundus too. However, there is one complication: Schmitt et al. [3] assumed the coherence length of the light source to be small compared to the mean free pathlength of the photons in the sample $1/\mu_t$. This allowed them to replace the coherence function γ by a Dirac delta function and, therefore, to avoid the solution of the integral in Equation (3). As can be seen from the values of μ_t in Table 1 and from the coherence length (13 μm), this is not possible in our case. Therefore, we had to solve the integral numerically.

Comparing the data in Table 1 with *in vitro* measurements from bovine retina and porcine choroids [13], we found complete agreement of the scattering anisotropy. However, the value of the extinction coef-

Table 1. Extinction coefficient and scattering anisotropy of retina and choroids

	μ_t	$\Delta\mu_t$	$\tilde{R}$	$\Delta\tilde{R}$	g	Δg
Retina	12 mm^{-1}	+120 mm^{-1}	0.0000407	+0.000061	0.97	−0.037
		−10.8 mm^{-1}		−0.0000407		+0.031
Choroids	27.5 mm^{-1}	+154 mm^{-1}	0.000146	+0.000292	0.90	−0.159
		−22 mm^{-1}		−0.000146		+0.104

ficient, which should be comparable to the scattering coefficient since absorption is nearly negligible at 855 nm, is about as double as high in the *in vitro* measurement than measured by OCT. This may be due to morphological differences between human and bovine or porcine tissues or, more likely, to rapid post mortem changes enhancing the opacity of the tissues. On the other hand, the differences between *in vivo* (OCT) and *in vitro* measurements are much smaller than the huge errors of the OCT-measurement resulting from the noise of the OCT signal.

The signal to noise ratio is principally limited by the photon shot noise. Additionally, the thermal noise of the detector and the electronic noise of the amplifier have to be considered. These broadband noise may be reduced by filtering the signal with the Doppler frequency f_D, whereas the bandwidth of the filter has to be at least $2v/\Delta$ if v is the speed of the reference mirror and a depth resolution Δ shall be achieved [14]. Furthermore, the coherent signal is affected by speckle. This could be reduced by an incoherent averaging over measurements at different wavelengths or by a local averaging which, however, reduces the resolution. Therefore, Schmitt et al. [15] used a detector array in order to reduce the speckle by averaging over measurements under slightly different angles. A further enhancement of the signal to noise ratio is possible if the observed depth plane z is always confocal to the detector. This requires a synchronization of the shift of the reference mirror with that of the focus. A solution of this problem is published by Lexer et al. [16].

The theory of single backscattering assumes complete loss of coherence after the second scattering event. The influence of multiple scattered light was estimated by Schmitt et al. [7] calculating the effective detector cross sections for single and multiple scattered light. For a specimen with optical properties similar to that reported here, they found a remarkable contribution of multiple scattered light for depths greater than 0.3 mm. Since the thicknesses of the retina and the choroid are smaller, the single scattering model can be regarded as sufficient for the description of the coherent signal.

Despite all problems mentioned above, the measurement of the extinction coefficient and of the anisotropy of scattering has shown to be possible. To get reliable values for the extinction coefficient, the signal to noise ratio of the measurement has to be improved substantially. The determination of the refractive indices should be possible too if the coherent reflection is measured in power units and is normalized to the incident power.

Acknowledgement

The authors would like to thank Prof. Fercher and his team for providing the data of the OCT-scan shown in Figure 1.

References

1. Huang D, Swanson EA, Lin CP, Schuman JS, Stinson WG, Chang W, Hee MR, Flott T, Gregory CA, Pulafito CA, Fujimoto JG. Optical coherence tomography. Science 1991: 254: 1178–1181.
2. Danielson BL, Whittenburg CD. Guided wave reflectometry with micrometer resolution. Appl Opt 1987; 26: 2836–2842.
3. Schmitt JM, Knüttel A, Bonner RF. Measurement of optical properties of biological tissues by low-coherence reflectometry. Appl Opt 1993; 32: 6032–6042.
4. Fercher A F, Mengedoht K, and Werner W (1988) Eye length measurement by interferometry with partially coherent light. Optics Letters 13: 186-189
5. Hitzenberger CK. Optical measurement of the axial eye length by laser Doppler interferometry. Invest Ophthalmol Vis Sci 1991; 32: 616–624.
6. Fercher AF. Optical coherence tomography. J Biomed Opt 1996; 1: 157–173.
7. Schmitt JM, Knüttel A, Grandjbakhche A, Bonner RF Optical characterization of dense tissue using low-coherence interferometry. Proc SPIE 1993; 1889: 197–211.
8. Yadlowsky MJ, Schmitt JM, Bonner RF. Multiple scattering in optical coherence microscopy. Appl Opt 1995; 34: 5699–5707.

9. Brent RP. Algorithms for Minimization without Derivatives. Prentice-Hall, Englewood Cliffs, 1973.
10. Henyey LG, Greenstein JL. Diffuse radiation in the galaxy. Astrophys J 1941; 93: 70–83.
11. Baumgartner A, Hitzenberger CK, Sattmann H, Drexler, W, Fercher F. Signal and resolution enhancement in dual beam optical coherence tomography of the human eye. J Biomed Opt 1998; 3: 45–54.
12. Naumann GOH. Pathologie des Auges, Bd. 1, Springer-Verlag, Berlin, Heidelberg, New York, 1997.
13. Hammer M, Roggan A, Schweitzer D, Müller G. Optical properties of ocular fundus tissues – an in vitro study using the double-integrating-spere technique and inverse Monte Carlo simulation. Phys Med Biol 1995; 40: 963–978.
14. Yadlowsky MJ, Schmitt JM, Bonner RF. Contrast and resolution in the optical-coherence microscopy of dense biological tissue. SPIE Proc 1995; 2387: 193–203.
15. Schmitt JM. Array detection for speckle reduction in optical coherence microscopy. Phys Med Biol 1997; 42: 1427–1439.
16. Lexer F, Fercher AF, Sattmann H, Drexler W, Molebny S. Dynamic coherent focus for transversal resolution enhancement of OCT. Proc SPIE 1998; 3251: 85–90.